Transient heat pump behaviour: a theoretical investigation

J. W. MacArthur

Key words: heat pumps, vapour compression heat pump, model

Comportement de la pompe à chaleur en régime transitoire: recherche théorique

On décrit un modèle mathématique détaillé de pompes à chaleur à compression. On donne des équations de modélisation des divers composants de la pompe à chaleur. Les composants modélisés comprennent le condenseur, l'évaporateur, l'accumulateur, le détendeur et le compresseur. On présente un bref examen des techniques de modélisation ainsi que la méthodologie de résolution. On présente aussi les résultats préliminaires de simulation. Le modèle établi permet de prévoir les valeurs spatiales de la température et de l'enthalpie en fonction du temps pour les deux échangeurs de chaleur. Les températures et les enthalpies de l'accumulateur, du compresseur et du détendeur sont modélisées suivant le processus des paramètres groupés. Les réponses de la pression sont déterminées à l'aide de modèles satisfaisants de continuité tant pour le condenseur que pour l'évaporateur. Le résumé donne une liste des travaux à venir prévus dans le domaine de la modélisation dynamique des pompes à chaleur.

A detailed mathematical model of vapour compression heat pumps is described. Model equations of the various heat pump components are given. The component models include the condenser, evaporator, accumulator, expansion device, and compressor. A brief discussion of the modelling techniques is presented, as is the solution methodology. Preliminary simulation results are also illustrated. The model developed predicts the spatial values of temperature and enthalpy as functions of time for the two heat exchangers. The temperatures and enthalpies in the accumulator, compressor and expansion device are modelled in lumped-parameter fashion. Pressure responses are determined by using continuity satisfying models for both the condenser and evaporator. The summary provides a list of future work anticipated in the area of dynamic heat pump modelling.

Nomenclature

A	area
C	specific heat, clearance volume, coefficient
d	differential operator
FF	constant
$f()$	functional relationship
h	enthalpy, surface heat transfer coefficient
$\bar{h}$	bulk surface heat transfer coefficient (hA)
J	spatial integration limit
m	mass
$\dot{m}$	mass flow rate
n	polytropic coefficient
p	pressure, perimeter
q	rate of heat flow
$\dot{r}$	removal rate (refrigerant mass)
S	Laplace operator
T	temperature
t	time
V	velocity, volume
v	specific volume
x	spatial distance
γ	isentropic coefficient
Δ	delta
∂	partial differential operator
ρ	density
η	efficiency
τ	time constant

Subscripts

c	condenser
e	evaporator
g	gas or vapour phase
hx	heat exchanger wall
i	i^{th} node, inlet, inside
l	liquid
o	outlet, outside
r	refrigerant
s	secondary fluid, shell
v	vapour

Superscripts

o	old value
'	new value

Conversion factors

$\frac{5}{9}(°F - 32) = °C$

mass flow rate 1 lb h^{-1} = 0.454 kg h^{-1}

heat flow rate 1 Btu h^{-1} = 0.293 W

The author is from Honeywell Inc., Technology Strategy Center, 1700 West Highway 36, Roseville, MN 55913, USA. Paper received 20 May 1983.

0140-7007/84/002123-10$3.00

© 1984 Butterworth & Co (Publishers) Ltd and IIR

Interest in heat pumps has increased significantly over the last decade. A substantial amount of research has been undertaken to improve the acceptance of the devices by the development of more efficient systems. A number of papers presented in one of a series of heat pump technology conferences held in Oklahoma have been documented.[1] Optimization of component and system design to increase energy efficiency is one of the major areas of interest.[2,3,4] Most ongoing research is currently concerned with the evaluation of steady or quasi-steady heat pump performance. Recently, hov - ever, there has been a thrust to investigate the effec. of system control on heat pump operation and the effect of integrated control on the operation of advanced heat pump systems. To perform these tasks requires a detailed understanding of the responses of the refrigerant system pressures, condenser and evaporator temperature profiles, compressor and expansion flows, and a host of other system parameters, particularly during off-design transient operation. Further, for closed-loop control synthesis, it is extremely important to know the response and stability characteristics of the overall system as well as its components.

Review of the literature shows that there has been important work in the area of dynamic heat pump modelling; some examples are given.[5-8] To perform the aforementioned tasks effectively required the development of a new model. It was the intention of this research effort to develop a flexible, detailed model based on first principles that is sophisticated enough to allow for a realistic representation of overall system response. The model developed is discussed below.

Heat pump model

Derivations of the heat pump equations will be given in the following paragraphs. First the generalized heat exchanger equations will be presented. Then each of the individual component models will be discussed. Numerical techniques for the solution of the governing equations will also be described.

The general heat exchanger equations used in this model are derived from the basic energy and continuity conservation equations:

$$\rho\frac{\partial h}{\partial t}+\rho V\frac{\partial h}{\partial x}+\frac{h_i p_i}{A}(T_t-T_{hx})=0 \qquad (1)$$

$$\frac{\partial \rho}{\partial t}+\frac{\partial \rho V}{\partial x}=0 \qquad (2)$$

The response of the secondary fluid is governed by:

$$\rho\frac{\partial h}{\partial t}-\rho V\frac{\partial h}{\partial x}-\frac{h_o p_o}{A}(T_{hx}-T_f)=0 \qquad (3)$$

$$\frac{\partial \rho}{\partial t}-\frac{\partial \rho V}{\partial x}=0 \qquad (4)$$

and the response of the heat exchanger wall is given by:

$$C\rho A\frac{\partial T_{hx}}{\partial t}-h_i p_i(T_r-T_{hx})+h_o p_o(T_{hx}-T_f)=0 \qquad (5)$$

Equations (1) through (5) define the heat exchanger response and are equally valid for either the condenser or evaporator. Although these equations represent counterflow operation, alternate flow geometries (such as crossflow) may be represented easily in a manner similar to that given above. The solution of (1) through (5) requires some information about the velocity or flow field. For the completely general case, this information is given by the momentum equation. For this model, certain assumptions that eliminate the need to solve the momentum equation have been imposed on the flow fields.

The model described in the following sections has been developed for use as a research tool. To ensure the greatest degree of flexibility, the model has been based solely on first principles. In essence, any desired response can be obtained by adjusting the appropriate parameters; therefore, no effort was made to fit the model to a particular set of heat pump data. Instead, parameter values that illustrate the significant features of the model, and that were felt to be representative of components in the range of those currently obtainable in the field, were used. The only heuristic or curve-fit data is that concerning the physical properties of the refrigerant and the correlations defining the surface coefficients. The following is a description of the modelling and solution methodology used for each of the components in the heat pump simulation.

Condenser

The condenser is modelled in two sections, the first to model the heat exchange and the second to model the pressure response. Heat exchanger response can be determined by discretizing the calculation domain into a series of control volumes, as shown in Fig.1 and integrating (1) through (5) over the appropriate control volumes with respect to time and distance.

The equations used to solve for the refrigerant in section one are:

$$\int_{t^0}^{t'}\int_{J-1}^{J}\rho\frac{\partial h}{\partial t}dx\,dt+\int_{t^0}^{t'}\int_{J-1}^{J}\rho V\frac{\partial h}{\partial x}dx\,dt+\int_{t^0}^{t'}\int_{J-1}^{J}\frac{h_i p_i}{A}(T_r-T_{hx})dx\,dt=0 \qquad (6)$$

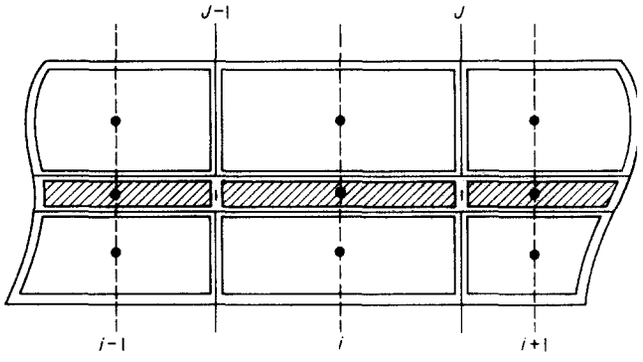

Fig. 1 Domain discretization

Fig.1 Discrétisation du domaine

and

$$\int_{t^0}^{t}\int_{J-1}^{J}\frac{\partial \rho}{\partial t}dxdt+\int_{t^0}^{t}\int_{J-1}^{J}\frac{\partial \rho V}{\partial x}dxdt=0 \qquad (7)$$

Equations (3) through (5) can be integrated in a similar fashion. For this model, the flow is assumed to be uniform and one dimensional along the length of the heat exchanger. The resulting equations are a set of fully implicit coupled equations defining the response of the i^{th} control volumes for the refrigerant, heat exchanger wall, and secondary fluid, respectively. The control volume formulation, as discussed by Patankar[9] yields exact balances for the appropriate conservation expressions. Thus, the implicit equations exactly satisfy energy and continuity conservation requirements for any grid spacing (Δx) or step size (Δt). Although energy and continuity balances are assured with the above formulation, the accuracy of the solution is indeed a function of both the step size and grid spacing. The effect of these key parameters on solution accuracy has been discussed[10] for various one- and two-dimensional energy transport applications.

The response of section two of the condenser is determined by assuming an adiabatic node at the end of the heat exchanger. The rsponse of this node is governed solely by continuity. Thus, the response of liquid and vapour refrigerant in the condenser is given by:

$$\frac{dm_l}{dt}=\dot{m}_{l_c}-\dot{m}_{l_x} \qquad (8)$$

$$\frac{dm_v}{dt}=\dot{m}_{v_i}-\dot{m}_{l_c}-\dot{m}_{v_x} \qquad (9)$$

where

$\dot{m}_{v_i}$ = inlet vapour flow;

$\dot{m}_{l_c}$ = liquid condensed along the heat exchanger;

$\dot{m}_{v_x}$ = vapour flow through expansion devices;

$\dot{m}_{l_x}$ = liquid flow through expansion devices.

Once the heat transfer along the length of the condenser is known, the exit quality and hence all terms on the right-hand side of (8) and (9) will be known. The pressure response can be determined based on the various masses, volumes and thermophysical property data of the refrigerant.

The refrigerant properties are modelled by general equations developed for the Freon refrigerants (R 11, 12, 13, 14, 21, 22, 23, 113, 114) by Martin[11] at the University of Michigan.

Solution of the condenser model is accomplished by using an iterative line-by-line[9] search for the temperature and enthalpy field at each time step. The direction of the search makes use of the fact that the Peclet number is infinite (no axial conduction).

After each expression has been evaluated, an updated temperature enthalpy field will exist. In general, this field will be approximate since the state at a given gridpoint is known only in terms of the states at other gridpoints, which are themselves unknown. Field accuracy is continuously increased by iterating the implicit equations. During each iteration, updated gridpoint values are substituted for the current gridpoint values. Iterations over the entire field continue until the updated values are equal (within a specified tolerance) to the current values.

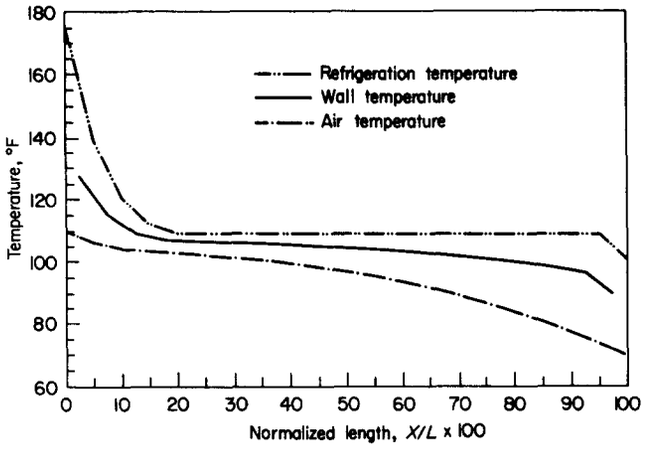

Fig. 2 Condenser temperature profiles at steady state (air entering condenser – 70°F; air entering evaporator=42°F)

Fig.2 Profils de température du condenseur en régime permanent (air entrant dans le condenseur à 21°C; air entrant dans l'évaporateur à 6°C)

Within each iteration for each grid point, nonlinearities are incorporated by calling the appropriate subroutine defining the nonlinearity. For example, the refrigerant temperature is determined by calling the refrigerant thermophysical properties routine with the condenser pressure and the current value of the enthalpy. Updating the current value of the enthalpy causes a corresponding change in the refrigerant temperature, which in turn causes the next update of the enthalpy to change. When the updated value of the enthalpy is equal to the current value, the refrigerant routine will give identical values for the refrigerant temperature on two successive calls, and the refrigerant temperature will no longer disturb the enthalpy calculation. At convergence, the temperature enthalpy field will no longer be changing and the refrigerant temperature will agree with the corresponding pressure and enthalpy at each grid point.

With the heat exchanger equations evaluated, the condenser pressure response is determined in an explicit fashion. Note that the condenser model utilizes both implicit and explicit formulations. In general, each of the routines or modules representing a specific heat pump component (ie, condenser, evaporator, accumulator, etc) may utilize either explicit or implicit formulation or any combination thereof. The executive program solves for overall system response by automatically interconnecting subsystem modules and integrating in an explicit manner. A description of this general-purpose program is given elsewhere.[12,13]

Fig.2 gives the steady-state temperature profiles for the condenser of a heat pump designed to give 36 000 Btu h^{-1} at the stated conditions. The profiles are plotted in terms of normalized distance, $\bar{X}$. Superheated refrigerant leaves the compressor at 176°F and enters the condenser at $\bar{X}=0$. The refrigerant is desuperheated, condensed, and subcooled approximately 8°F. Seventy-degree air enters the condenser at $\bar{X}=100$, flows through the heat exchanger, and leaves at 110°F.

Evaporator

An effective evaporator model is one that can predict both the vapour and liquid flows, the stored refrigerant mass, and the temperature and enthalpy profiles during transient and steady-state operation. It is convenient in the development of a model with these features to represent the single- and two-phase regions separately. The response of the vapour and liquid refrigerant is governed by the expressions:

$$\frac{\partial m_v h_g}{\partial t} = \dot{m}_e h_v - \frac{\partial \dot{m}_v h_g}{\partial x} dx \quad (10)$$

$$\frac{\partial m_l h_l}{\partial t} = h_i p_i dx (T_{hx} - T_r) - \frac{\partial \dot{m}_l h_l}{\partial x} dx - \dot{m}_e h_v \quad (11)$$

$$\frac{\partial m_v}{\partial t} = - \frac{\partial \dot{m}_v}{\partial x} dx + \dot{m}_e \quad (12)$$

$$\frac{\partial m_l}{\partial t} = - \frac{\partial \dot{m}_l}{\partial x} dx - \dot{m}_e \quad (13)$$

Here it is assumed that the vapour and liquid are in temperature equilibrium and that the heat transfer from the heat exchanger wall is used to evaporate refrigerant at the rate $\dot{m}_e$. The response of the single-phase region is given by (1) and (2). Note that the bulk enthalpy in the two-phase region can be determined by substituting (11) into (10). This substitution will yield an expression identical to that given by (1) when similar substitutions are made for the continuity equation.

The final evaporator model can be obtained by discretizing the above equations in both the spatial and time co-ordinates in a manner similar to that discussed in the previous paragraphs.

Equations (12) and (13) can be used to define the enthalpy along the evaporator. However, these equations give the total enthalpy, including that of the flowstream and the stored mass. At start-up there will be significant amounts of stored liquid along the evaporator and/or accumulator in the form of pools of refrigerant. Usually the enthalpy of concern is that associated with the fluid flowstream. This enthalpy is given by the expression:

$$h_i = (\dot{m}_{v_i} h_g + \dot{m}_{l_i} h_l) / (\dot{m}_{v_i} + \dot{m}_{l_i}) \quad (14)$$

for two-phase flow. In the single-phase region, the enthalpy is given by:

$$m_i \frac{dh_i}{dt} = \dot{m}_{i-1} h_{i-1} - \dot{m}_i h_i - h A_i (T_{r_i} - T_{hx_i}) \quad (15)$$

Solution of these equations requires some information on the flow field. For this model the information is obtained in the form of an enthalpy constraint. The enthalpy at each node is calculated by two different equations, one given by (14), the other by the expression:

$$h_i = (1 - m_{l_i} / (\rho_{l_i} Vol_i)) h_{fg} + h_l \quad (16)$$

When the nodal mass reaches an equilibrium condition, (16), (14) and (15) give identical values for h_i. During initial transient operation, the nodal enthalpy given by (16) and (14) can be different as (14) is concerned only with the flowing refrigerant. Thus, the solution strategy is to first assume that the liquid level in the evaporator is uniform. With this assumption the appropriate flows and enthalpies are calculated. Once the flow enthalpy, given by (14), becomes less than the enthalpy given by (16), an iterative procedure is used to calculate the flow field, which satisfies (14) and (16). Unlike the condenser model, the evaporator model requires the calculation of the liquid refrigerant distribution.

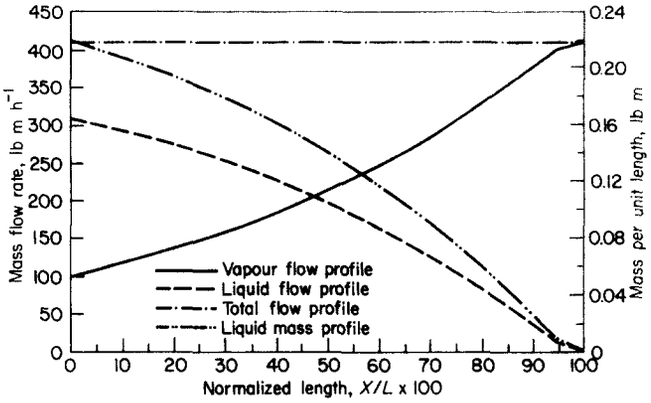

Fig. 3 Evaporator mass and flow profiles at steady state

Fig.3 Profils de masse et d'écoulement dans l'évaporateur en régime permanent

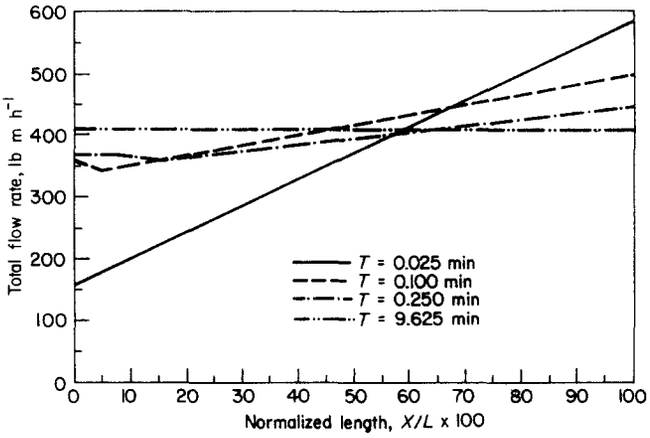

Fig. 4 Total evaporator flow profiles as a function of time

Fig.4 Profils des débits globaux de l'évaporateur en fonction du temps

The equations defining the response of the evaporator wall and secondary fluid are identical to those given in the description of the condenser model.

During steady-state operation, the evaporator usually will have a region containing two-phase refrigerant and a region containing single-phase superheated refrigerant. Heat that is transferred in the two-phase region simply converts liquid refrigerant into vapour. As the liquid refrigerant is evaporated in the flow direction, the vapour flow rate increases. The increase in the vapour flow rate corresponds directly to a decrease in the liquid flow rate, and the sum of the flows is a constant under equilibrium conditions.

Heat that is transferred to the single-phase region superheats the refrigerant vapour. The location of the two-phase superheat interface is defined by the point at which the mass of liquid is equal to zero. For the conditions given in Fig.3, the interface resides in the last node. Note that the actual location of the interface is at $X = 97.2$; thus, almost the entire heat exchanger is used to evaporate the refrigerant.

Under transient operation, the sum of the liquid and vapour flows changes dramatically. This is borne out by Fig.4. Here the total flow at 0.025 minutes varies from 162 lb m h^{-1} at the entrance to 591 lb m h^{-1} at the exit. The entrance flow is determined by the flow passed through the expansion device, and the exit flow is determined by the inlet flow and the amount of refrigerant evaporated along the heat exchanger. At the beginning of the on period, the expansion flow is at a minimum and the exit flow reaches maximum after only a few seconds of operation. Hence, the rate of change of the flow profile is greatest during system start-up. At equilibrium conditions, the flow through the valve must equal the flow through the compressor, which requires that the slope be equal to zero and that the total flow be constant.

The response of the liquid mass in the evaporator as a function of time is given in Fig.5. Initially, the liquid level is uniform along the length of the heat exchanger. This corresponds to periods of pool-type boiling. As the condenser pressure increases and the evaporator pressure decreases, the inlet enthalpy to the evaporator will decrease. This decrease in inlet enthalpy corresponds to an increase in inlet liquid refrigerant flow, which causes a build-up of liquid refrigerant in the upstream section of the evaporator. As time passes, this fluid 'front' moves in the downstream direction. At approximately 2.4 min, the 'front' covers about 65% of the heat exchanger. The evaporator, however, remains flooded at this time. At 3.9 min (not shown in Fig.12), the liquid mass at $X = 100$ is completely evaporated and the two-phase vapour interface begins to move into the heat exchanger. At this point, the evaporator is no longer flooded. At 9.625 minutes, the heat pump is at equilibrium and the mass profile is the same as that given in Fig.8 for steady-state operation.

The temperature response of the evaporator during an on and off cycle is illustrated in Fig.6. All temperatures experience a rapid decrease during the first half minute of operation. During this time, the compressor rapidly 'sucks down' the evaporator pressure. Because the evaporator is flooded, the saturated refrigerant temperature tracks the evaporator pressure. The evaporator temperature experiences a minimum point at 0.6 min. This 'undershoot' is caused by the inability of the evaporator to vaporize refrigerant at a rate compatible

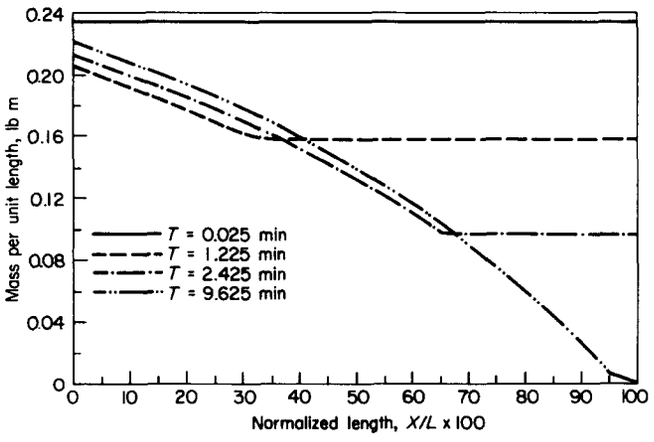

Fig. 5 Evaporator liquid mass profiles as a function of time

Fig.5 Profils de masse de liquide de l'évaporateur en fonction du temps

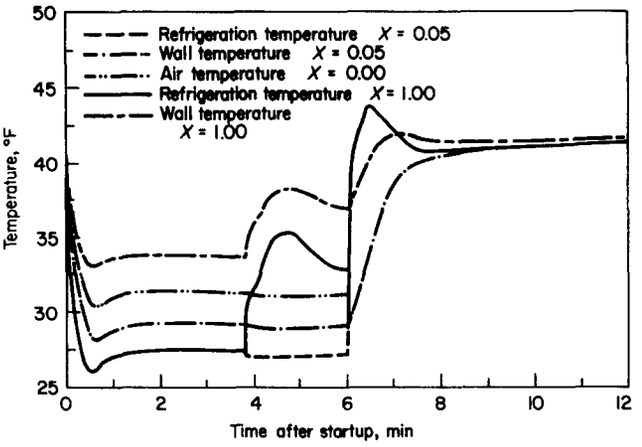

Fig. 6 Evaporator temperature response during an on/off cycle

Fig.6 Réponse de la température de l'évaporateur au cours du cycle tout ou rien

with the vapour pumping capacity of the compressor during the initial start-up transient. This mismatch is further aggravated by the decrease in available flash gas from the expansion device during the same time period.

At 3.9 min, enough liquid has been evaporated to allow the exit conditions of the evaporator to become superheated. As the two-phase vapour interface moves into the heat exchanger, the exit refrigerant temperature increases rapidly. The evaporator pressure drops slightly under exit superheat conditions due to reduced vapour generation along the length of the heat exchanger. During the off period, the refrigerant temperature and pressure increase rapidly. This rapid response is due to the fact that the compressor is off; therefore, no vapour is removed from the evaporator, while at the same time, vapour continues to flow into the evaporator due to flashing of the liquid refrigerant in the condenser. Once all of the liquid has been flashed from the condenser, pure vapour flows at a drastically reduced rate. This effect is evidenced by the inflection in the refrigerant temperature just before the temperature reaches its maximum value. During the off period, the refrigerant in the evaporator is assumed to be fully mixed; the heat exchanger wall, however, still has a temperature distribution. Depending on that distribution, heat will flow into or out of the refrigerant, and eventually all temperatures will reach the source temperature of 42°F. After approximately 7 min, the heat transfer process is driven by airside natural convection; thus, the time required to reach equilibrium is relatively long.

Accumulator

The accumulator is assumed to be located directly downstream from the evaporator. The accumulator entrance conditions are the same as the evaporator exit conditions, and the accumulator exit conditions are the same as the compressor entrance conditions. The accumulator is represented by a lumped-parameter model and is shown schematically in Fig.7.

The energy and continuity equations for the vapour are:

$$\frac{dmh}{dt} = \dot{m}_v h_v + \dot{m}_e h_g + h_{iv}(T_w - T_v) - \dot{m}_c h \qquad (17)$$

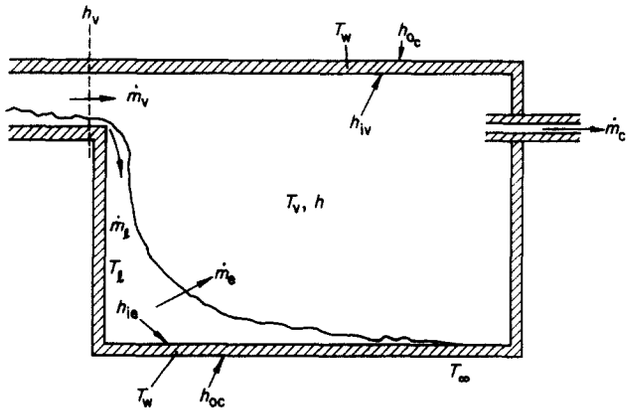

Fig. 7 Schematic representation of the accumulator

Fig.7 Représentation schématique de l'accumulateur

$$\frac{dm_v}{dt}=\dot{m}_v+\dot{m}_e-\dot{m}_c \tag{18}$$

and for the liquid are:

$$\frac{dmh_l}{dt}=\dot{m}_l h_l-\dot{m}_e h_g+h_{il}(T_w-T_l) \tag{19}$$

$$\frac{dm_l}{dt}=\dot{m}_l-\dot{m}_e \tag{20}$$

where h_V is equal to h_g when the exit conditions of the evaporator are saturated. Solution of these equations requires iteration within each time step. The method used is similar to that discussed in the condenser subsection, except here there is no spatial direction. The pressure response of the evaporator and accumulator can be calculated by determining the total mass of liquid and vapour refrigerant residing in the evaporator and accumulator at any instant in time. The total mass of vapour is given by:

$$m_{v_T}=(\dot{m}_v-\dot{m}_c+\dot{m}_e)\Delta t+m^{\circ}_{v_T} \tag{21}$$

and the total mass of liquid is given by:

$$m_{l_T}=\sum_{i=1}^{N} m_{l_i}+(\dot{m}_l-\dot{m}_e)_{acc}\Delta t+m^{\circ}_{l_T} \tag{22}$$

This information, together with the available internal volumes, allows the pressure calculations to proceed in a straightforward fashion.

Compressor

Fig.8 is a schematic representation of the compressor and depicts the key states necessary to define the compressor response. Fig.9 is a pressure-enthalpy diagram of the compressor illustrating the same states as those shown in Fig.8. Operation of the compressor can be described in terms of five parameters: clearance factor (C); piston displacement (PD); compression efficiency (η); heat transfer coefficient (h); and thermal mass (ρV).

Refrigerant leaving the accumulator enters the compressor at state one. This refrigerant interacts with the casing and external cylinder walls and is usually superheated as it enters the suction valve at state two. The enthalpy of the refrigerant at this state is given by the expression:

$$\rho V\frac{dh_2}{dt}=\dot{m}_c(h_1-h_2)+\bar{h}_{c_o}(T_c-T_2)-\bar{h}_{s_{l_i}}(T_2-T_{s_{l_i}})+q_m \tag{23}$$

where the cylinder and shell temperatures (T_c and T_{s_1}) are given by the expressions:

$$(C\rho V)_c\frac{dT_c}{dt}=\bar{h}_{c_i}(T_5-T_c)-\bar{h}_{c_o}(T_c-T_2) \tag{24}$$

and

$$(CpV)_{s_1}\frac{dT_{s_1}}{dt}=\bar{h}_{s_{1_i}}(T_2-T_{s_1})-\bar{h}_{s_{1_o}}(T_{s_1}-T_\infty) \tag{25}$$

On the suction stroke, the refrigerant experiences a pressure drop, Δp_{v_1}, across the inlet valve, and is then compressed from state three to state four. The pressure at state four must be greater than the condenser pressure by the amount Δp_{v_2}, which is the pressure drop experienced by the refrigerant as it flows through the discharge valve.

The specific volume and enthalpy for isentropic compression are:

$$v_{4_s}=v_3\Big/\left(\frac{p_4}{p_3}\right)^{1/\gamma}$$

$$h_{4_s}=f(v_{4_s}, p_4)$$

The actual enthalpy and temperature of state four expressed in terms of a compression efficiency are:

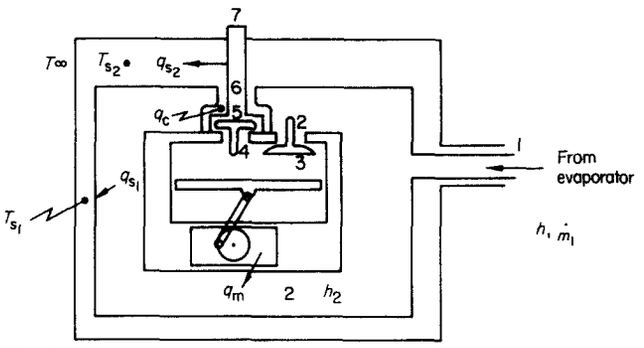

Fig. 8 Compressor schematic

Fig.8 Représentation schématique du compresseur

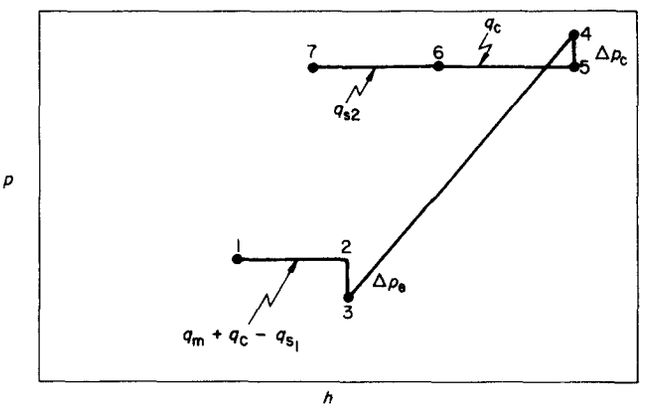

Fig. 9 Pressure-enthalpy diagram

Fig.9 Diagramme pression-enthalpie

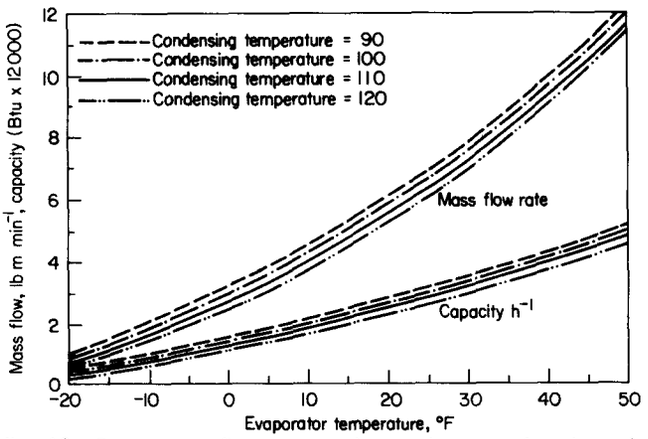

Fig. 10 Compressor flow rate and capacity as a function of evaporating and condensing temperatures (0° subcool, 10° superheat)

Fig.10 Débit et puissance du compresseur en fonction des températures d'évaporation et de condensation (0°C: sous-refroidissement, 5,5°C: surchauffe)

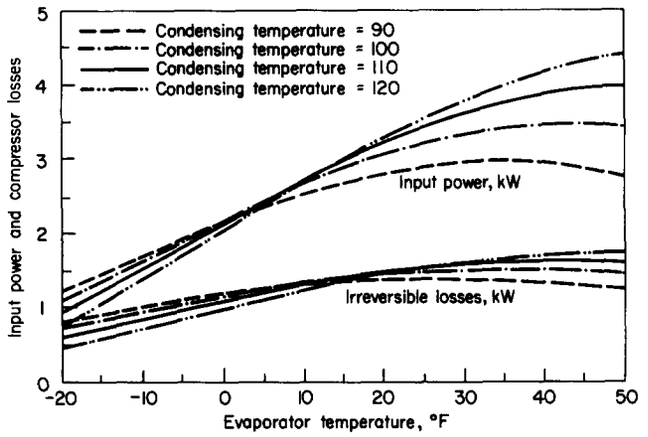

Fig. 11 Compressor input power and irreversible losses as a function of evaporating and condensing temperatures (0° subcool, 10° superheat)

Fig.11 Puissance consommée par le compresseur et pertes irréversibles en fonction des températures d'évaporation et de condensation (0°C: sous-refroidissement, 5,5°C: surchauffe)

$$h_4 = h_3 + (h_{4_s} - h_3)/\eta$$

$$T_4 = f(h_4, p_e)$$

As the refrigerant flows past the discharge valve, the pressure drops and the new state can be determined based on state four.

At this point, heat is assumed to be transferred to the cylinder wall. It is assumed that heat is also transferred from the refrigerant to the compressor shell at the discharge section of the compressor, where the upper shell temperature is defined by the expression:

$$(C\rho V)_{s_2}\frac{dT_{s_2}}{dt} = q_{s_2} - \bar{h}_{s_{2_o}}(T_{s_2} - T_\infty) \qquad (26)$$

The compressor states at each time step are determined by sequentially evaluating the governing equation. Equations (23) through (26) are solved by integrating in an explicit manner. The compressor flow rate is assumed to be polytropic; therefore, it is calculated by the expression:

$$\dot{m}_c = \frac{PD}{v_3}\left(1 + C - C\left(\frac{P_4}{P_3}\right)^{\frac{1}{n}}\right) \qquad (27)$$

where n is the polytropic coefficient defined in terms of gamma as:

$$n \equiv \gamma - FF(\gamma - 1)$$

and gamma is a function of the suction entropy.

The steady-state operation of the compressor is illustrated in Figs 10 and 11, in terms of mass flow, system capacity, input power, and compressor losses. These parameters are plotted as a function of evaporating and condensing temperatures. Fig.12 shows the dynamic response of the compressor for an on and off cycle.

Expansion device

There are a number of different throttling devices available for use between the condenser and evaporator. Two types, the fixed orifice valve and the thermostatic expansion valve (TEV), have been modelled in this study. A block diagram of the TEV valve is shown in Fig.13.

Flow through the TEV and the fixed orifice valve is represented by the orifice equation:

$$\dot{m} = C_1 A_t (\rho \Delta p)^{0.5} \qquad (28)$$

In the TEV model, the time response of the valve is included in the time constant, τ, of the thermobulb. Although both types of devices have been modelled, the model of the fixed orifice valve (A_t=constant) has been used to generate all the heat pump data found in this paper. Note that the expansion devices modelled in this program do not currently account for choked/-sonic flow conditions. However, future work is planned to develop a more refined model that will incorporate more complex flow phenomena.

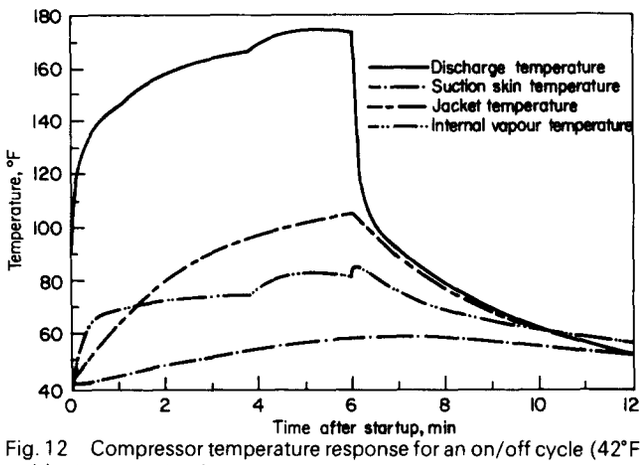

Fig. 12 Compressor temperature response for an on/off cycle (42°F ambient temperature)

Fig.12 Réponse de la température du compresseur pour un cycle tout ou rien (température ambiante de 6°C)

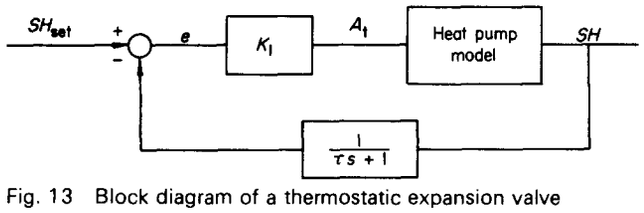

Fig. 13 Block diagram of a thermostatic expansion valve

Fig.13 Organigramme d'un détendeur thermostatique

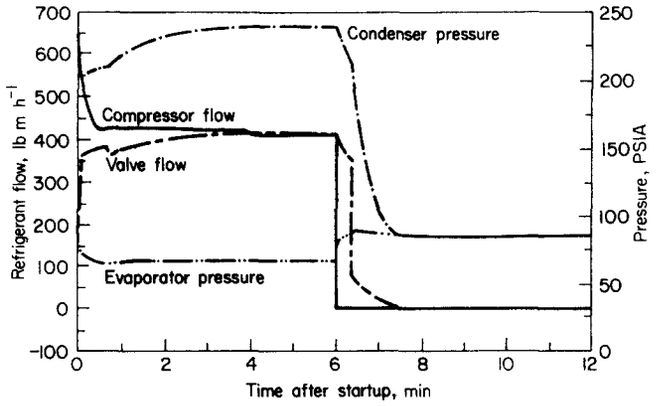

Fig. 14 Heat pump pressure and mass flow response for an on/off cycle

Fig.14 Réponse des pressions et débits de la pompe à chaleur pour un cycle tout ou rien

System response

The response of the overall heat pump system can be determined by coupling the component models into an overall system model. The responses of the various components shown in the preceding figures were, in fact, generated in this manner, but were presented on an individual basis for clarity. The parameters to be discussed here are the system pressures, charge inventory and the mass and energy flows. Fig.14 shows the mass flow and pressure response for the heat pump operating at the conditions discussed previously.

Before the start of the on cycle, the evaporator and condenser pressures are in equilibrium at 86 psia. For the first 0.1 min of the cycle, the condenser pressure rises very rapidly, while the evaporator pressure decreases. During the same time period, the compressor flow decreases from a maximum value at the start of the cycle (this assumes an instantaneous torque output of the motor driving the compressor) to about 545 lb m h^{-1}, while the valve flow increases from zero to approximately 310 lb m h^{-1}. The distinct flattening of the pressure response curve at 0.1 min is caused by the subcooled condition at the condenser exit. The rise in the condenser pressure during the next half minute is due to the decreased volume available for the vapour as the volume required by the liquid increases. The flattening in the condenser pressure response causes a similar flattening in the mass flow through the valve. At approximately 0.8 min, the condenser exit conditions become saturated. As the discharge condenser quality increases, the inlet density to the valve decreases, thus, the valve flow decreases. Concurrently, the vapour pressure in the condenser increases. As the condenser pressure continues to rise, the valve flow begins to increase. After 3 min, the pressures and flows are almost at their equilibrium condition. At 3.9 min, the superheat disturbance at the evaporator exit causes the compressor flow to decrease. The system approaches its final steady-state operating condition at 6 min. Here the valve flow is 410 lb m h^{-1}, which equals the flow through the compressor. The condenser and evaporator pressure at 241 and 66 psia, respectively.

During the off period, the liquid residing in the receiver initially is flashed through the valve; hence, the flow is driven by the inlet liquid density and the pressure difference between the condenser and evaporator. When there is no longer any liquid in the receiver, vapour begins to flow. At this point in time, the flow is driven by the inlet vapour density, which is 50 to 60 times smaller than that of liquid density. Thus, there is a discrete drop in the valve flow as the inlet condition changes from liquid to vapour. Because the flow through the compressor is assumed to be equal to zero during the off period, all the mass that flows through the valve tends to raise the pressure in the evaporator and decrease the pressure in the condenser. Two minutes after shutdown, the heat pump is almost at its equilibrium off-cycle condition. At equilibrium, the flows are equal to zero and the condenser and evaporator are both at the saturation pressure given by the source temperature, in this case 86 psia (42°F).

The refrigerant charge distribution during an on and off cycle is given in Fig.15 in terms of the vapour and liquid mass residing in the high (condenser, receiver, discharge) and the low (evaporator, accumulator, suction) sides of the system. To satisfy continuity, the sum of all vapour and liquid masses should always be constant and equal to the system charge. This figure illustrates that the continuity constraint is exactly satisfied, even though there are flow discontinuities during the on/off transition.

To satisfy energy constraints, the net energy flow must be identically equal to zero at equilibrium con-

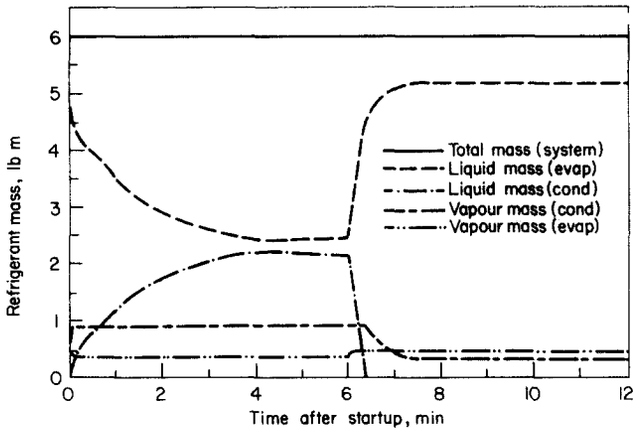

Fig. 15 Refrigerant charge distribution during an on/off cycle

Fig.15 Répartition de la charge de frigorigène pendant le cycle tout ou rien

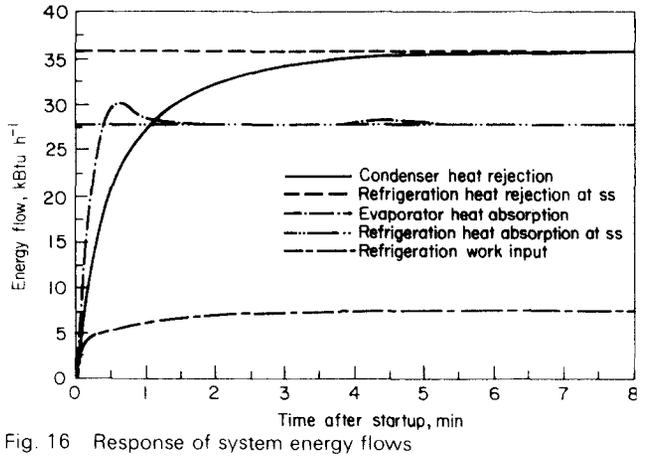

Fig. 16 Response of system energy flows

Fig.16 Réponse des flux énergétiques du système

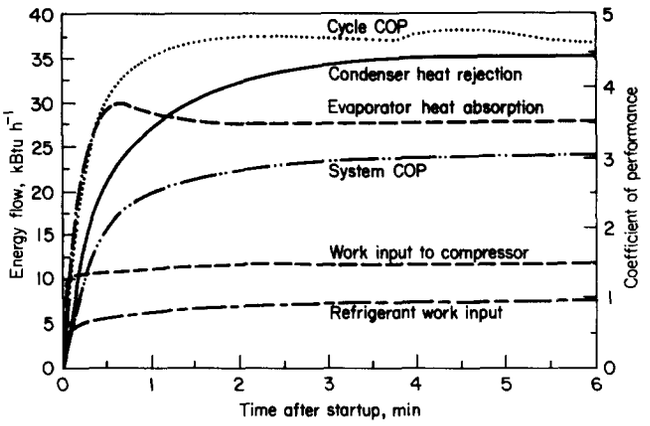

Fig. 17 System response during pickup

Fig.17 Réponse du système pendant le fonctionnement

ditions. Fig.16 gives the response of the various energy flows of the system. The condenser heat rejection and evaporator heat absorption represent the energy gained and lost by the secondary fluids in the condenser and evaporator, respectively. The refrigerant heat rejection and absorption represent the energy lost and gained by the refrigerant in the condenser and evaporator, respectively, under equilibrium conditions. Under steady-state operating conditions, the heat rejected by the refrigerant in the condenser is the same as the heat absorbed by the secondary fluid. Further, the energy rejected by the condenser is equal to the energy absorbed by the evaporator plus the energy input to the refrigerant in the compressor. Thus, the energy constraints are exactly satisfied for the entire system.

Fig.17 shows the heat pump system response during pickup in terms of the heat rejected and absorbed, the work input to the compressor and refrigerant, and the system and cycle coefficient of performance (*COP*). The rejection and absorption rates refer to the secondary fluids and are the same as those given in the previous figure.

Summary

A basic analysis describing the dynamic interaction of vapour compression heat pumps has been presented. The analysis was developed using a fundamental approach in that the equations developed were based on conservation principles. The current model has been internally verified, that is, it is internally consistent and therefore satisfies all conservation constraints. Since it was the intent of the first phase to develop a sound preliminary model based on first principles, little effort has been made to validate it against specific heat pump data. Although the validation effort is important, a sound physical model is crucial for an effective analysis. Even without validation, a sound model can yield quite satisfactory results (see Table 1). A model that is not internally consistent, however, can be validated (adjusted to fit specific data) and yet violate basic principles. Rather than adjust specific coefficients to ensure that the analysis 'fit' laboratory data at a given condition, a comprehensive validation effort will be conducted during the next phase of this research effort, such that the empirical data used will be applicable over a broad

Table 1. Comparison between model and laboratory data for source and sink temperatures of 42° and 70°F, respectively

Tableau 1. Comparaison entre le modèle et les résultats de laboratoire pour une température de la source froide de 6°C et une température de rejet de chaleur de 21°C

Parameter	Model	Data
Heat rejection, Btu h^{-1}	35 760	35 500
Input power, kW	3.44	3.5
Mass flow, lbm h^{-1}	410	415
Condensing temperature, °F	109	110
Evaporating temperature, °F	27	29
Discharge operation, °F	176	180
Suction superheat, °F	5.8	10.0
Heat delivery time constant, min	0.55	0.50
System *COP* (no auxiliary)	3.03	2.97

range. This approach will allow the model to be useful at conditions other than those at which the correlations were established.

In addition to validation, work is also planned in the refinement of the preliminary model, specifically in the area of improved heuristic data such as the correlations that define the heat transfer coefficients. The inclusion of the time-dependent momentum equation and associated pressure drop calculations will also be addressed. Other areas to be studied in future research include: treatment of oil migration/mixture in the refrigerant; dynamic first principle frost model; flow reversal; alternate prime movers (ie, heat engines versus electric motors); and advanced controls, local loop (ie, advanced flow controls) or system (ie, optimizer).

Use of the model described herein hopefully will aid in the development of more effective heat pump controls by providing a better understanding of the dynamic heat pump operation.

References

1 Heat pump technology conference, Tulsa, Oklohama; sponsored by OSU Extension, Oklahoma State University (1982)

2 **Ellison, R. D., Creswich, F. A.** 'A computer simulation of steady-state performance of air-to-air heat pumps, Oak Ridge National Laboratory Report ORNL/CON-1G (1978)

3 **Bonne, U., Patani, A.** 'Modelling the influence of heat pump sizing, climate and test conditions on seasonal efficiency, Conference on HVAC Equipment and Systems, Purdue University, West Lafayette, Indiana (October 23–25, 1978)

4 **Rice, C. K., et al.** 'Design optimization of conventional heat pumps: application to steady-state heating efficiency *ASHRAE Trans* **80** 11 (1973)

5 **Dhar, M., Soedel, W.** Transient analysis of a vapor compression refrigeration system. XV International Congress of Refrigeration, Venice, Italy (1979)

6 **Lee, W., Bonner, S. A., Leonard, R. G.** Dynamic analysis and simulation of a gas regular, Proc Int Symp on Flow, its Measurement and Control, ISA, Pittsburgh, Pennsylvania (May 1971)

7 **Chi, J., Didion, D.** A simulation model of the transient performance of a heat pump *Int J Ref* **5** 3 (1982)

8 **Bonne, U., Patani, A., Jacobson, R., Muller, D.** Electric-driven heat pump system: simulation and controls *ASHRAE Trans* LA-80-5 **4** Los Angeles, California (May 1980)

9 **Patankar, S. V.** Numerical heat transfer and fluid flow, McGraw-Hill, New York (1980)

10 **MacArthur, J. W., Meixel, G. D., Shen, L. C.** Application of numerical methods for predicting energy transport in earth contact systems *J Appl Energy* **13** (1983)

11 **Martin, J. J.** Correlations and equations used in calculating the thermodynamic properties of Freon refrigerants, ASME, New York, New York (1959)

12 **MacArthur, J. W., Benton, R., Mahesh, J. K.** Generalized engineering modelling and simulation tool--GEMS, Honeywell Final Report, Vol. I, II, III (1981)

13 **Benton, R., MacArthur, J. W., Mahesh, J. K., Cockroft, J. P.** Generalized modeling and simulation software tools for building systems *ASHRAE Trans* **88** 11 (1982)